

Illumination and Measurement Precision for Lunar Photography

The precision of photogrammetric measurements made on Apollo metric camera photographs deteriorated as the angle between the sun and the local horizontal increased.

INTRODUCTION

MAPPING CAMERAS, panoramic cameras, and laser altimeters were installed in the Scientific Instrument Modules (SIM) of Apollos 15, 16, and 17 for the purpose of accurately mapping part of the Moon. The

of the metric camera system, a precise timing device, and a laser altimeter with a ranging resolution capability of 1 m (Light, 1972; National Space Science Data Center, 1972, 1973, 1974). Metric camera photographs from these three missions, in conjunction

ABSTRACT: *Illumination is an important factor affecting the precision of stereo-photogrammetric measurements made on Apollo metric camera photographs of the lunar surface. Large angles between the sun and the local horizontal result in a low-contrast image producing relatively poor precision. The same result is obtained for very small angles where the measured area is in diffuse shadow, and no measurements can be made in black shadows. Lunar surfaces illuminated with sun elevation angles below 10° have a large percentage of area in shadow. In general, the optimum angle between the sun and the local horizontal for good precision is between 10° and 30°.*

Angles between planes of local surfaces and the sun also affect the precision of measurements. Precision of measurements on surfaces tilted at large angles toward the sun are poorer than those tilted from a few to 30° toward the sun.

Average standard errors of elevation measurements for Apollo metric photographs taken with sun elevation angles near 10° to 30° are 7 to 10 m and, for sun elevation angles near 80°, are 14 to 16 m. The same results are obtained for the angles between the sun and tilted surfaces. The data show considerable scatter, reflecting variations in contrast resulting from the heterogeneous lunar surface.

The lunar results differ from those for Earth photography for which sun elevation angles near 45° are optimal. These results should be considered in planning future missions to the Moon with planned imaging and photographic experiments as well as those to other planetary bodies such as Mars.

mapping camera system for each mission included a 76-mm focal length metric terrain camera with a ground resolution of 15-20 m at an altitude of 110 km, a 76-mm focal length stellar camera for absolute orientation

with these auxiliary devices, provide not only a capability for producing a selenodetic control net (Light, 1972) but also the capability for producing 1:250,000-scale topographic maps with a contour interval of 100 m

(see, for example, Defense Mapping Agency, 1974a). High-resolution panoramic cameras, which are not discussed here, were also included in the mapping camera system and provided the capability for producing large-scale topographic maps with relative contour intervals of 10 to 20 m (see, for example, Defense Mapping Agency, 1974b) and detailed profiles (see, for example, Moore and Schaber, 1975).

The photography from the metric cameras of the three missions covers approximately 20 per cent of the lunar surface and is an important data base for selenodesy, lunar geology, lunar gravity studies, and other scientific endeavors. Because of the scientific importance of the metric camera photog-

raphy, the effect of illumination conditions on the precision or standard error of measurements using photogrammetric techniques is examined in this study.

Apollo metric camera photographs provide an excellent opportunity for such a study because nearly identical cameras and the same type of film were used in each mission. Thus, other variables were reduced to a minimum. Preliminary studies, which included panoramic camera photography, have been reported previously (Wu *et al.*, 1973).

The results from this study can provide constraints on interpretations of maps prepared from metric camera photographs, are useful as a guide for photograph selection from the existing Apollo metric camera

TABLE IA. EXPERIMENTAL CONDITIONS AND RESULTS FOR PRECISION OF MEASUREMENTS OF APOLLO 15 METRIC CAMERA PHOTOGRAPHY. STANDARD ERROR IS ESTIMATE OF PRECISION¹.

Photograph number	Location		Sun angle (°)		Number of points measured	Standard error (m)				Terrain type
	Lat.	Long.	Photograph	Model		Single photograph	All points	Central column		
1849	25°N	38°W	2.4	1.8	34 of 35(a)	7.10	7.75	6.77	Smooth	
1850			1.2		34 of 35	8.41		6.71		
1853	25°S	124°E	8.5	9.2	33 of 35(b)	8.79	7.95	8.83	Rugged	
1854			9.8		30 of 35	7.10		6.87		
1861	23°S	114°E	18.7	19.3	35 of 35	7.06	6.72	7.26	Rugged	
1862			19.9		35 of 35	6.38		7.05		
1869	20°S	103°E	28.5	29.2	35 of 35	7.64	7.17	8.68	Rugged	
1870			29.8		35 of 35	6.69		6.15		
1877	15°S	94°E	38.5	39.1	35 of 35	9.65	8.63	9.34	Rugged	
1878			39.7		35 of 35	7.62		6.24		
1886	10°S	83°E	49.6	50.2	35 of 35	10.06	9.07	8.84	Rugged	
1887			50.8		35 of 35	8.07		8.14		
1894	5°S	73°E	59.3	59.9	35 of 35	13.64	13.86	15.56	Rugged	
1895			60.5		35 of 35	14.09		12.53		
1903	1°N	64°E	69.5	70.2	35 of 35	12.35	12.02	13.94	Rugged	
1904			70.9		35 of 35	11.69		12.31		
1913	6°N	53°E	79.4	79.4	35 of 35	15.08	13.94	17.91	Mixed	
1914			79.5		35 of 35	12.81		9.32		
1933	17°N	30°E	68.1	67.5	35 of 35	11.36	9.77	8.32	Mixed	
1934			66.9		35 of 35	8.18		6.70		
1943	22°N	16°E	56.2	55.6	29 of 29	9.89	9.48	8.20	Mixed	
1944			54.9		30 of 30(b)	9.08		9.69		
1849	25°N	38°W	2.4	1.8	34 of 35(a)	7.78	7.56	7.01	Smooth	
1850			1.2		34 of 35	7.34		8.02		
1933	17°N	30°E	68.1	67.5	35 of 35	13.68	14.00	16.61	Mixed	
1934			66.9		35 of 35	14.32		14.75		

¹ Photograph numbers are grouped as stereopairs. Selenographic coordinates and sun elevation angles are from the photographic support data for principal points of each photograph (National Space Science Data Center, 1972, 1973, 1974). Sun elevation angle for stereomodel is estimated. Number of points are listed as those measured of total points available: (a) indicates number of points measured was reduced because of black shadow; (b) indicates number of points measured was reduced because of relatively small photograph overlap or obscuration by part of spacecraft; no letter indicates all of planned points were measured. Standard errors are (a) average for all points measured near reseau marks in each photograph of stereopair, (b) average for points near reseau marks of central column on each photograph, and (c) average for all points measured on both photographs of stereomodel. Terrain types are classed into two types: upland or rugged terrain and mare or smooth terrain. Some stereo-models had mixtures of the two types of terrain.

photographs, and have value in the planning of future photographic lunar exploration missions. The study should also be useful for planning imaging and photographic missions to other planetary bodies with little or no atmosphere.

EXPERIMENTAL CONDITIONS AND PROCEDURES

Thirty-five metric camera stereomodels were used in this study. Eleven models from Apollo 15, starting at 25°S, 124°E and proceeding westward to 25°N, 38°W (Department of Defense, 1973), cover rugged upland terrain at the start and end with coverage of mare areas (Table 1a). Ten models from Apollo 16, starting at 8°N, 146°E and proceeding westward to 9°S, 11°W (Defense Mapping Agency, 1972), are chiefly in rugged upland terrain except near 1°N, 87°E and at the end, which cover mare areas (Table 1b). Fourteen models from Apollo 17, starting at 19°S, 154°W and proceeding westward to 23°N, 10°W (Defense Mapping Agency, 1973), begin in rugged upland terrain and end in smooth maria (Table 1c).

Stereomodels with sun elevation angles ranging from about 1° to 86° and with approximately 10° difference in sun elevation between successive individual models were selected to give a wide and continuous range of illumination conditions (see Table 1a, 1b, and 1c). In the study, where the angle between the local surface and the sun direction was used in analyses, the angles ranged between about 1° and 87°.

Measurements were made using an AP/C analytical plotter (Ottico Meccanica Italiana, 1966) and master positive transparencies. The master positive transparencies are the best quality reproductions available and are the original format size giving a model scale near 1:1.5 million. Overlap between successive metric camera photographs was near 78 per cent, but it varies somewhat so that base-to-height ratios were between 0.3 to 0.4 (National Space Science Data Center, 1972, 1973, 1974). The AP/C plotter has a least significant reading of 1 μ m. Repeated measurements with the AP/C have a precision near $\pm 2\mu$ m. When combined with the scale and base-height ratios of the metric camera

TABLE 1b. EXPERIMENTAL CONDITIONS AND RESULTS FOR PRECISION MEASUREMENTS OF APOLLO 16 METRIC CAMERA PHOTOGRAPHY. STANDARD ERROR IS ESTIMATE OF PRECISION.

Photograph number	Location		Sun angle(°)			Standard error (m)			Terrain type
	Lat.	Long.	Photograph principal point	Model center	Number of points measured	Single photograph (35 pts)	Model	Central col. of photograph	
AS16-									
1287			2.0		54 of 70 ^a	8.38		8.35	
1288	9°S	11°W	0.8	1.4	54 of 70 ^a	7.88	8.13	8.31	Smooth
1850			10.9		68 of 70 ^a	7.59		7.62	
1851	8°N	146°E	12.2	11.6	66 of 70 ^a	5.53	6.56	4.89	Rugged
1857			19.8		70 of 70	10.05		10.45	
1858	7°N	137°E	21.0	20.4	70 of 70	8.86	9.46	7.38	Rugged
1865			29.8		70 of 70	11.00		12.46	
1866	6°N	127°E	31.3	30.5	70 of 70	9.31	10.16	8.13	Rugged
1873			39.9		70 of 70	7.95		9.85	
1874	5°N	117°E	41.1	40.6	70 of 70	9.34	8.64	8.53	Rugged
1880			48.7		70 of 70	14.83		15.04	
1881	4°N	108°E	50.0	49.3	70 of 70	12.21	13.52	11.10	Rugged
1889			59.8		70 of 70	16.74		15.73	
1890	3°N	97°E	61.2	60.6	70 of 70	12.90	14.82	11.37	Rugged
1897			69.9		70 of 70	13.02		14.64	
1898	1°N	87°E	71.1	70.5	70 of 70	12.87	12.95	11.10	Smooth
1905			79.6		70 of 70	19.31		21.70	
1906	1°S	77°E	80.7	80.2	70 of 70	14.19	16.75	10.82	Rugged
1912			86.1		70 of 70	17.02		18.48	
1913	2°S	68°E	86.1	86.1	70 of 70	15.73	16.38	15.85	Rugged

Note: Measured points are twice those of Apollo 15 because they were paired to yield local slopes.

photographs used in this study, this precision translates to ± 7.5 m to ± 10 m. The film had a resolution of 200 lines/mm, but actual photos had a ground resolution of about 20m. Probable errors for single readings are about 1/5 to 1/6 of the resolution or 1.2 to 3.8m (Gardner, 1932). When combined with the scale and base-height ratios of the metric camera photographs used in this study (Doyle, 1963), the probable error translates to ± 4.2 to 5.4 m.

Orientations, sun elevation angles, and selenographic coordinates for the principal points of the photographs were obtained using photographic support data (National Space Science Data Center, 1972, 1973, 1974). Although the photographic support

data may have small errors, they have little or no effect on the results described below.

Three elevation readings were made for each point. The general scheme was to select areas for measurement of points near 35 planned reseau marks, as shown on Figure 1. Elevation readings could not always be made near the 35 reseau marks because of reduced overlap of the stereopairs along the flight line, obscuration by hardware of other experiments, and areas that were completely shadowed. Deviations from the general scheme are noted in Table 1a, 1b, and 1c. For Apollo 15, the points measured were single points that usually totaled 35 for each photograph or 70 for each stereomodel. For Apollo 16 and 17, the points were measured

TABLE 1C. EXPERIMENTAL CONDITIONS AND RESULTS FOR PRECISION MEASUREMENTS OF APOLLO 17 METRIC CAMERA PHOTOGRAPHY. STANDARD ERROR IS ESTIMATE OF PRECISION.

Photograph number	Location		Sun angle ($^{\circ}$)		Number of points measured	Standard error (m)			Terrain type	
	Lat.	Long.	Photograph principal point	Model center		Single photograph (35 pts.)	Model	Central col. of photograph		
AS17-										
0169	19 $^{\circ}$ S	154 $^{\circ}$ W	1.0	1.6	30 of 70	(a)	8.70	9.64	5.82	Rugged
0170			2.2		34 of 70		10.57		10.24	
0177	18 $^{\circ}$ S	165 $^{\circ}$ W	11.2	11.9	58 of 70	(a)	10.62	10.81	11.94	Rugged
0178			12.5		64 of 70		11.01		12.60	
0185	16 $^{\circ}$ S	176 $^{\circ}$ W	21.6	22.2	64 of 70	(a)	8.74	8.26	8.90	Rugged
0186			22.9		64 of 70		7.77		8.02	
0192	14 $^{\circ}$ S	174 $^{\circ}$ E	30.7	31.3	70 of 70		8.63	8.01	8.90	Rugged
0193			32.0		70 of 70		7.39		6.96	
0199	12 $^{\circ}$ S	166 $^{\circ}$ E	39.9	40.5	64 of 64	(b)	7.95	8.16	6.60	Rugged
0200			41.2		64 of 64		8.37		8.50	
0207	8 $^{\circ}$ S	156 $^{\circ}$ E	50.4	51.0	64 of 64		8.39	8.49	9.68	Rugged
0208			51.7		64 of 64		8.60		6.12	
0215	5 $^{\circ}$ S	145 $^{\circ}$ E	60.8	61.4	64 of 64	(b)	9.41	9.43	9.41	Rugged
0216			62.1		64 of 64		9.44		7.12	
0223	2 $^{\circ}$ S	136 $^{\circ}$ E	71.0	71.7	68 of 68	(b)	13.93	13.08	15.30	Rugged
0224			72.3		64 of 64		12.23		10.10	
0231	2 $^{\circ}$ N	126 $^{\circ}$ E	80.5	81.0	66 of 66	(b)	10.96	11.44	11.16	Rugged
0232			81.5		60 of 60		11.91		10.42	
0236	4 $^{\circ}$ N	119 $^{\circ}$ E	84.7	84.6	54 of 54	(b)	26.64	24.70	27.41	Rugged
0237			84.4		60 of 60		22.77		21.79	
1229	20 $^{\circ}$ N	15 $^{\circ}$ E	13.7	13.1	70 of 70		6.93	6.67	9.20	Smooth
1230			12.4		70 of 70		6.40		7.02	
2919	23 $^{\circ}$ N	25 $^{\circ}$ W	18.8	18.4	70 of 70		8.99	8.90	10.88	Smooth
2920			18.0		70 of 70		8.81		8.66	
2279	23 $^{\circ}$ N	10 $^{\circ}$ W	21.0	20.4	70 of 70		9.16	8.99	10.73	Smooth
2280			19.8		70 of 70		8.82		8.66	
2908	23 $^{\circ}$ N	10 $^{\circ}$ W	32.6	32.0	70 of 70		7.38	7.98	9.78	Smooth
2909			31.4		70 of 70		8.59		8.29	

Note: Measured points are twice those of Apollo 15 because they were paired to yield local slopes.

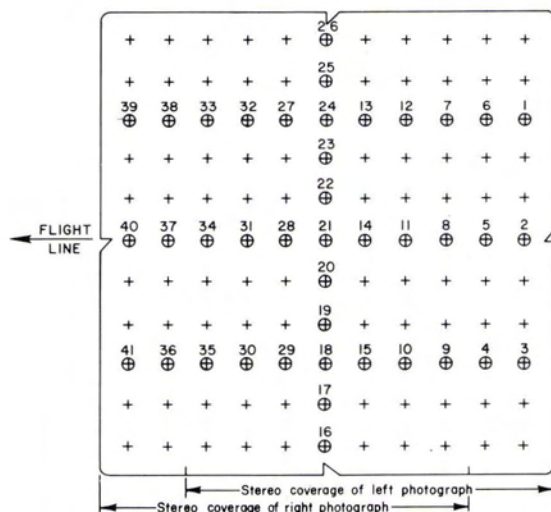


FIG. 1. Diagram showing location of reseau marks where repeated elevation measurements were made for estimates of precision or standard errors. Because of overlap, 35 points were usually measured on each photograph. For one photograph, points 7 through 41 were measured. For the second photograph, points 1 through 35 were measured. Reseau marks on models were never superposed. Deviations from this general plan are noted in Table 1a, 1b, and 1c.

in pairs separated by 500 to 800 m along a line parallel to the flight line. There were generally 35 pairs for each photograph or 140 for each stereomodel. The paired points were used to calculate local slopes. For Apollo 16 these slopes are a good approximation of the tilt of the local surface in the direction of the sun because the orbit was nearly equatorial. For Apollo 17, the approximation is not so good because of the inclined orbit and components of slope may be in error by as much as 15 to 20 per cent. This condition occurred where sun elevation angles were the largest for the mission.

Standard errors for each point were calculated from the three measurements using the well-known formula

$$S = \pm \sqrt{\frac{\sum_{i=1}^n (\bar{Z} - Z_i)^2}{n - 1}}$$

where S is the standard error, n is the number of elevation readings at each point, Z_i is an elevation reading, and \bar{Z} is the mean of the three elevation readings. Because the elevation measurements at each point are made without disturbing the horizontal position, elevation is the only variable in the

error analysis of precision. Standard errors for a larger number of points are averaged for (1) the entire stereomodel, (2) points corresponding to each photograph in the stereomodel, and (3) those along the central columns of each photograph. These average values are listed in Table 1a, 1b, and 1c and represent the estimate of precision.

RESULTS AND ANALYSIS

The data for all three missions show a clear dependence between measured standard errors and sun elevation angles. Although there is considerable scatter in the data, average standard errors for stereomodels with sun elevation angles below 30° are near 7 to 10 m and comparable to the nominal standard error expected for the AP/C plotter (Figures 2, 3, 4, and 5; Tables 1a, 1b, and 1c). Average standard errors for the largest sun elevation angles are about twice those for the low sun elevation angles and exceed the AP/C nominal standard error. Thus, it is clear that measurement precision generally decreases with increasing sun elevation angle for Apollo metric camera photographs.

Inspection of the high sun elevation angle photographs reveals a poorer quality of image than those taken at lower sun eleva-

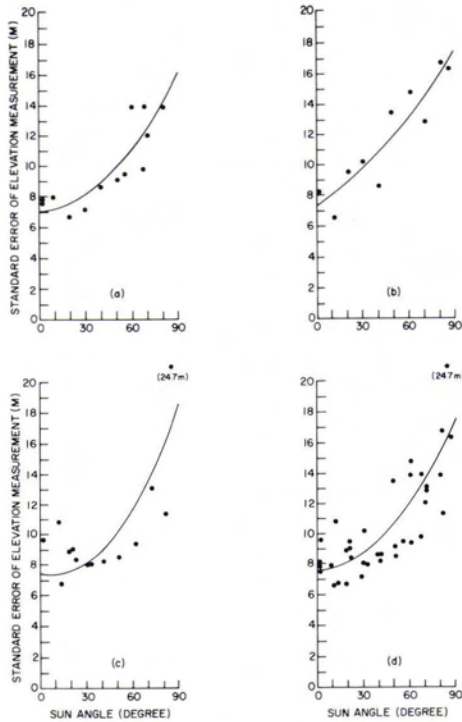


FIG. 2. Regression curves determined from average standard errors of measurement for each stereomodel and average sun elevation angle for each stereomodel. Dots indicate values used for regression fits to (a) Apollo 15 data, (b) Apollo 16 data, (c) Apollo 17 data, and (d) data from all three missions combined.

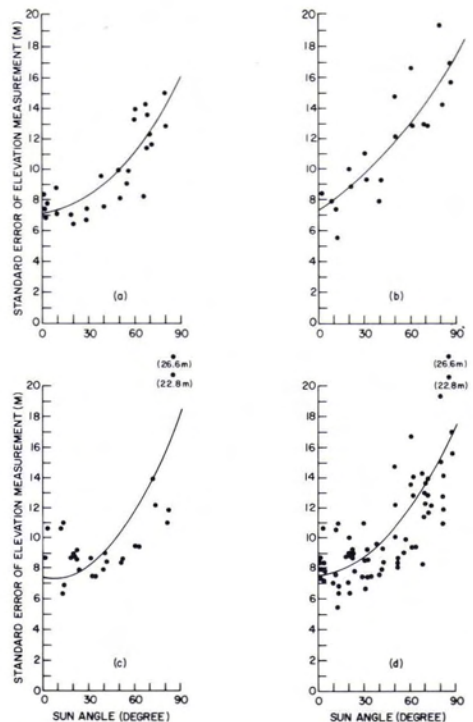


FIG. 3. Regression curves determined from average standard errors of measurement for individual photographs and average sun elevation angles of each photograph. Dots indicate values used for regression fits to (a) Apollo 15 data, (b) Apollo 16 data, (c) Apollo 17 data, and (d) data from all three missions combined.

tion angles. This degradation is caused by the photometric function of the Moon because other photographic parameters were nearly the same. Indeed, contrast in some areas of high sun elevation angle photographs was so poor that the surface could not be measured. For very low sun elevation angles less than about 10° , some points could not be measured because they were in black shadow (Tables 1a, photographs #1849 through 1854; Table 1b, photographs #1287 through 1851; Table 1c, photographs #0169 through 0186). In one area of rugged upland more than 57 per cent of the points could not be measured. Thus, low sun elevation angles obscure significant amounts of surface by shadow, but for sun elevation angles greater than about 10° , less than 28 per cent of rugged surfaces are obscured.

Analytical relations between standard errors and sun elevation angles were obtained from the data for each mission and all three missions combined by using (1) average

standard errors for all of the measured points in the stereomodel and the sun elevation angle for the model (Table 2 and Figure 2), (2) average standard errors for all of the measured points associated with each photograph of the stereopair and the sun elevation angle for the corresponding principal point of each photograph (Table 3 and Figure 3), and (3) average standard errors for all of the measured points associated with the central column of each photograph of the stereopair and the sun elevation angle of corresponding principal point of each photograph (Table 4 and Figure 4). In addition, analytical relations were obtained using (1) standard errors for individual measured points and local sun elevation angles for the measured points (Table 5 and Figure 5) and (2) standard errors for individual measured points and angle of tilt of the local surface with respect to the approximate direction of the sun (Table 6 and Figure 5). The approximation for Apollo 16 is good because of the

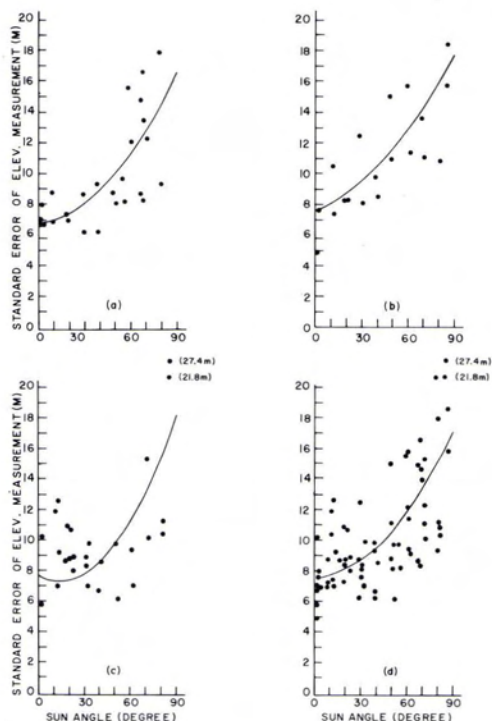


FIG. 4. Regression curves determined from average standard errors of measurements for central column of each photograph and average sun elevation angle for each photograph. Dots indicate values used for regression fits to (a) Apollo 15 data, (b) Apollo 16 data, (c) Apollo 17 data, and (d) data from all three missions combined.

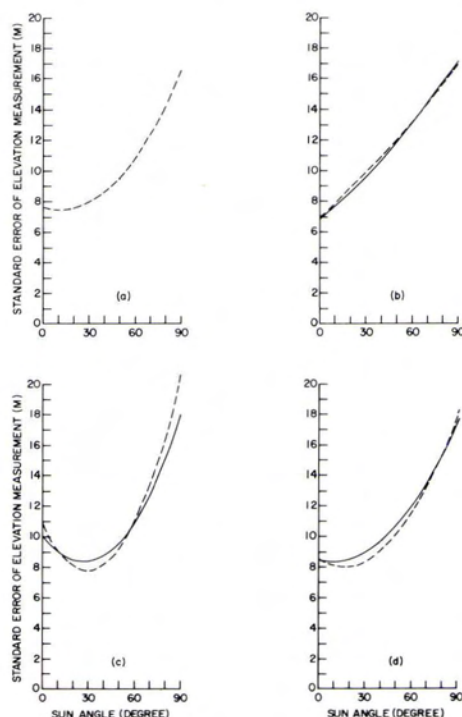


FIG. 5. Regression curves determined from standard error of measurement and local sun elevation angles (solid lines) and standard error of measurement and local sun elevation angles corrected for surface tilt (dashed lines) (a) for Apollo 15 data, (b) for Apollo 16 data, (c) for Apollo 17 data, and (d) for data from all three missions.

nearly equatorial orbit. For Apollo 17 the approximation is not so good, and slope errors near 15 to 20 per cent may be present.

Analytical fits were made by least-squares regression to a second degree curve (Steel and Torre, 1960, p. 161-193)

$$Y = \alpha + \beta X + \gamma X^2 \tag{2}$$

where Y is the standard error of measurement; X is the sun elevation angle; and α , β , and γ are coefficients determined by least-squares regression. Results are plotted in Figure 2 through 5 and listed in Tables 2 through 6. Correlation coefficients were calculated using (Spiegel, 1961, p. 217-268)

$$r = \sqrt{1 - \frac{\hat{S}_{y,x}^2}{S_y^2}} \tag{3}$$

where r is the correlation coefficient; $\hat{S}_{y,x}$ is a measure of the scatter about the regression

line of standard error on sun angle, i.e., the standard error of estimate of Y on X ; and S_y is the standard error of measurement (total residual). Standard errors of estimate of Y on X for the regressions ($\hat{S}_{y,x}$) were obtained using

$$\hat{S}_{y,x} = \pm \sqrt{\frac{\sum(Y - Y_e)^2}{n - 3}} \tag{4}$$

where Y is the standard error of measurement, Y_e is the value of standard error of measurement computed for a given sun elevation angle using equation (2), and n is the number of values of standard error of measurement. The standard error of Y (total residual) was estimated by:

$$\hat{S}_y = \pm \sqrt{\frac{\sum(\bar{Y} - Y_i)^2}{n - 1}} \tag{5}$$

where \hat{S}_y is the standard error of Y (total residual), \bar{Y} is the average standard error of

TABLE 2. COEFFICIENTS OF REGRESSION CURVES DETERMINED FROM AVERAGE STANDARD ERRORS OF EACH STEREO MODEL (Y) AND SUN ELEVATION ANGLES OF EACH MODEL (X). STANDARD ERROR OF Y ON X, STANDARD ERROR OF Y, CORRELATION COEFFICIENTS, AND NUMBER OF POINTS FITTED ARE ALSO LISTED.

Coefficients or parameters of regression curve	Apollo 15 mission	Apollo 16 mission	Apollo 17 mission	Combination of Apollo 15, 16, 17 missions
α , Constant term	7.13	7.33	7.41	7.51
β , Coefficient of 1st deg. term	0.00432	0.0646	-0.0253	0.00866
γ , Coefficient of 2nd deg. term	0.00106	0.000533	0.00165	0.00114
$\hat{S}_{x,y}$, Standard error of Y_{est} on $X(m)$	1.58	1.57	3.27	2.29
\hat{S}_y , Standard error of Y, total residual (m)	2.76	3.62	4.45	3.68
r , Correlation coefficient	+0.819	+0.900	+0.678	+0.783
n , Number of pts. fitted	13	10	14	37

TABLE 3. COEFFICIENTS OF REGRESSION CURVES DETERMINED FROM THE AVERAGED STANDARD ERROR OF EACH PHOTOGRAPH (Y) AND AVERAGE SUN ELEVATION ANGLE OF EACH PHOTOGRAPH (X). STANDARD ERRORS OF Y ON X, STANDARD ERROR OF Y, CORRELATION COEFFICIENTS, AND NUMBER OF POINTS FITTED ARE ALSO LISTED.

Coefficient or parameters of regression curve	Apollo 15 mission	Apollo 16 mission	Apollo 17 mission	Combination of Apollo 15, 16, 17 missions
α , Constant term	7.13	7.34	7.41	7.52
β , Coefficient of 1st deg. term	0.00421	0.0654	-0.0250	0.00863
γ , Coefficient of 2nd deg. term	0.00106	0.000521	0.00165	0.00114
$\hat{S}_{x,y}$, Standard error of y_{est} on $X(m)$	1.60	1.98	3.16	2.40
\hat{S}_y , Standard error of Y, total residual (m)	2.76	3.74	4.42	3.75
r , Correlation coefficient	+0.815	+0.847	+0.700	+0.767
n , Number of pts. fitted	26	20	28	74

TABLE 4. COEFFICIENTS OF REGRESSION CURVES DETERMINED FROM THE AVERAGE STANDARD ERRORS OF THE CENTRAL COLUMNS OF EACH PHOTOGRAPH (Y) AND SUN ELEVATION ANGLES FOR EACH PHOTOGRAPH (X), STANDARD ERROR OF Y ON X, STANDARD ERROR OF Y, CORRELATION COEFFICIENTS, AND NUMBER OF POINTS FITTED ARE ALSO LISTED.

Coefficient or parameters of regression curve	Apollo 15 mission	Apollo 16 mission	Apollo 17 mission	Combination of Apollo 15, 16, 17 Missions
α , Constant term	6.87	7.50	7.65	7.56
β , Coefficient of 1st deg. term	0.00500	0.0432	-0.0510	0.00403
γ , Coefficient of 2nd deg. term	0.00113	0.000769	0.00185	0.00114
$\hat{S}_{x,y}$, Standard error of Y_{est} on $X(m)$	2.47	2.80	3.65	3.01
\hat{S}_y , Standard error of Y, total residual (m)	3.41	4.19	4.60	4.11
r , Correlation coefficient	+0.690	+0.739	+0.608	+0.680
n , Number of pts. fitted	26	20	28	74

TABLE 5. COEFFICIENTS OF REGRESSION CURVES DETERMINED FROM ALL STANDARD ERRORS AND LOCAL SUN ELEVATION ANGLES FOR EACH MEASURED POINT.

Coefficients or parameters of regression curve	Apollo 15 mission	Apollo 16 mission	Apollo 17 mission	Combination of Apollo 15, 16, 17 missions
α , Constant term	7.70	6.91	10.84	8.48
β , Coefficient of 1st deg. term	-0.0361	0.0938	-0.206	-0.561
γ , Coefficient of 2nd deg. term	0.00149	0.000194	0.00348	0.00181
$\hat{S}_{x,y}$, Standard error of y_{est} on $X(m)$	3.194	4.020	3.782	3.780
\hat{S}_y , Standard error of Y , total residual (m)	3.925	5.033	5.045	4.724
r , Correlation coefficient	0.581	0.602	0.661	0.600
n , Number of cols. fitted	232	177	237	646

TABLE 6. COEFFICIENTS OF REGRESSION CURVES DETERMINED FROM INDIVIDUAL STANDARD ERRORS AND CORRECTIONS FOR LOCAL SUN ELEVATION ANGLES AND SURFACE TILTS.

Coefficients or parameters of regression curve	Apollo 15 mission	Apollo 16 mission	Apollo 17 mission	Combination of Apollo 16 & 17 missions
α , Constant term	No slopes were measured	7.00	10.02	8.42
β , Coefficient of 1st deg. term		0.0807	-0.125	-0.0214
γ , Coefficient of 2nd deg. term		0.000374	0.00236	0.00138
$\hat{S}_{x,y}$, Standard error of Y_{est} on $X(m)$		6.515	5.935	6.238
\hat{S}_y , Standard error of Y , total residual (m)		7.200	6.492	6.850
r , Correlation coefficient		+0.426	+0.405	+0.413
n , Number of cols. fitted		680	881	1,561

measurement, and Y_i are individual values of standard error of measurement. Correlation coefficients, standard errors for the regression, and standard errors of standard error of measurements are listed in Tables 2 through 6.

DISCUSSION

Two factors related to illumination condition are important considerations for selecting and planning lunar photography for the photogrammetric purposes: (1) the amount of area shadowed and unusable and (2) the effect of high sun elevation angles on image contrast. Sun elevation angles less than about 10° can result in an excessive amount of area in black shadow and areas of diffuse shadow where image contrast is reduced. Some parts of the lunar surface, such as the Censorinus Highlands, are very rugged and have average slopes near 8° at slope lengths of 500 m (Wu and Moore, 1972). For such rugged surfaces, as much as 27 per cent of the slopes measured parallel to the sun di-

rection are larger than 10° so that large percentages of the surface are lost in shadow. This loss of area is shown by the reduced number of points available for measurement in the low sun elevation angle photographs used in this study (Tables 1a, b, c). Additionally, inspection of the Apollo 17 low sun elevation angle photographs (Table 1c, photograph number 0169-0170 and 0177-0178) shows that one-third of the points, which were in partial to diffuse shadow, had standard errors from 10 to 26 m. These values are the chief contributors to the average standard errors of 9.64 m and 10.81 m, although a few bright slopes had large standard errors. Thus, the negative value of the coefficient β for Apollo 17 regression curves is produced by shadows. Lack of a negative β coefficient for the Apollo 15 and 16 regression curves may be the result of chance or a selection process on the part of the AP/C plotter operator for these two missions.

Large sun elevation angles produce poorer precision because of reduced contrast. The

large increase in reflected sunlight or *heiligschein* (see, for example, Wildey, 1972) reduces the contrast in the scene. For this condition, measurement precision exceeds the standard errors attributable to the AP/C plotter and the resolution of the photography. Similar results occur when local slopes are tilted toward and away from the sun. Those tilted toward it have reduced contrast when compared to those tilted away from it except when shadowed.

Regression curves fitted to the data for which nominal sun elevation angles were used are basically similar (Figures 2a, b, c). The coefficient α for all curves is near 7 to 7.5m. The coefficient β is negative for Apollo 17 and positive for the other two missions; all curves show an increase in standard error with increased sun elevation angle. For the regression curves fitted to the data that take the local sun elevation and, then, the local sun elevation and surface tilt into account, the coefficient β has a large effect for Apollo 17 and a weak one for Apollo 15, and the end result is a condition where the optimum sun elevation angle is near 10° to 30° .

Correlation coefficients are all positive, between 0.918 and 0.405, and demonstrate a relation between standard error of measurement and the average sun elevation angle for the model. Regression curves fitted to data for which local sun elevation angles and local surface tilts are considered are similar to those considering nominal sun elevation angles, and, therefore, support the dependence between standard error, sun angles, and surface tilt.

For almost all photographs on which the sun elevation angles were high, average measured standard errors were less than ± 25 m. This number is within the standard error of elevation when the error is calculated using the formula (Light, 1972; Doyle, 1963)

$$\sigma_h = S_p \left(\frac{H}{B}\right) \sigma_x \quad (6)$$

where σ_h is the standard error in elevation, S_p is the photograph scale factor, $\frac{H}{B}$ is the height-base ratio, and σ_x is the standard error of parallax measurement. For the conditions used in this study, σ_h nominally ranges between 7 m to 16 m. Since contour interval is usually chosen to be equal to or larger than $3\sigma_h$, then a contour interval of 50 m is feasible. Also, actual contouring could be done with alternate rather than consecutive photographs, thus providing base-height ratios of larger than 0.6. This could possibly allow an even smaller contour interval on an AP/C analytical plotter.

CONCLUSIONS

Standard errors measured on Apollo metric camera photography of the Moon strongly correlate with the illumination conditions. When sun elevation angles are less than about 10° , large areas are covered by shadow. This condition precludes measurements in the shadows, and standard errors in diffuse shadows tend to be large. Sun elevation angles increasingly larger than 30° are accompanied by increasing standard errors of measurements. Thus, the optimum sun elevation angles for photographs and images intended for photogrammetric measurement are between 10° and 30° . This result contrasts with those for the Earth for which optimum sun elevation angles are near 45° (Harmon *et al.* 1966, p. 211).

Similar results to those above are obtained where local slopes and sun direction are considered. Larger standard errors are measured on slopes tilted toward the sun and smaller standard errors are measured on slopes tilted away from the sun provided they are not shadowed.

Standard errors measured on Apollo photographs with large sun elevation angles rarely exceed a value of three-tenths the contour interval (100 m) used for most lunar topographic maps at 1:250,000 scale.

The results of this study can be used as a guide for the selection of photographs with optimum quality from existing Apollo metric camera photography, for planning future photographic missions to the Moon, and for planning future imaging and photographic missions to Mars.

ACKNOWLEDGMENTS

The author wishes to thank Dr. Henry J. Moore for his valuable suggestions and critical review. The author also wishes to thank Francis J. Schafter, Raymond Jordan, and Gary Nakata for their diligent, competent, and skillful efforts in collecting the data necessary for this study. The work was performed as part of NASA Experiment S-222.

REFERENCES

- Department of Defense, 1973, Apollo Mission 15 Lunar Photography Index Maps: Defense Mapping Agency Aerospace Center, St. Louis AFS, Missouri 63118, 10 sheets.
- Defense Mapping Agency, 1972, Apollo Missions 16 Lunar Photography Index Maps: Defense Mapping Agency Aerospace Center, St. Louis AFS, Missouri 63118, 6 sheets.
- , 1973, Apollo Mission 17 Lunar Photography Index Maps, prepared and published by the Defense Mapping Agency Aerospace

- Center, St. Louis AFS, Missouri 63118, for Natl. Aeronautics and Space Admin., 8 map sheets.
- _____. 1973, Apollo Mission 17 Lunar Photography Index Maps: Defense Mapping Agency Aerospace Center, St. Louis AFS, Missouri 63118.
- _____. 1974a, Lunar Topographic Orthophoto map (La Hire), LTO 40A4 (250), 1 sheet.
- _____. 1974b, Lunar Topophotomap (Apollo 16 Landing Area), LTO 78 D2 S1(50), 1 sheet.
- Doyle, F. J., 1963, the Absolute Accuracy of Photogrammetry: *Photogrammetric Engineering*, v. 29, p. 105-108.
- Gardner, I. C., 1932, The Optical Requirements of the Airplane Mapping: *Bureau of Standard Jour. of Research*, v. 8, p. 445-455.
- Harmon, W. E., Jr., R. H. Miller, S. W. Park, and J. P. Webb, 1966, Aerial Photography in M. M. Thompson, ed.: *Manual of Photogrammetry*, 3rd ed., v. 1, American Society of Photogrammetry, 536 p.
- Light, D. A., 1972, Photogeodesy from Apollo: *Photogrammetric Engineering*, v. 38, p. 574-587.
- Moore, H. J., and G. G. Schaber, 1975, An Estimate of the Yield Strength of the Imbrium Flows: Proc. Sixth Lunar Sci. Conf., *Geochim. Cosmochim. Acta Suppl.* 6, v. 1, p. 101-118.
- National Space Science Data Center, 1972, *Apollo 15 Lunar Photography*: National Space Science Data Center, Goddard Space Flight Center, NASA, Greenbelt Md., Data Users Note, NSSDC 72-07, 58 p.
- _____. 1973, *Apollo 16 Lunar Photography*: National Space Science Data Center, Goddard Space Flight Center, NASA, Greenbelt, Md., Data Users Note NSSDC 73-01, 60 p.
- _____. 1973, *Apollo 16 Lunar Photography*: National Space Science Data Center, Goddard Space Flight Center, Greenbelt, Md., NSSDC-73-01, 47 p. 2 appendices.
- _____. 1974, *Apollo 17 Lunar Photography*: National Space Science Data Center, Goddard Space Flight Center, NASA, Greenbelt, Md., Data Users Note, NSSDC 74-08, 68 p.
- Ottico Meccanica Italiana S.P.A., 1966, Analytical Plotter-Model AP/C, OMI 66-An, 181×7, 81 Via Della Vasca Navale, Rome, Italy, 77 p.
- Spiegel, M. R., 1961, *Theory and Problems of Statistics*, Schaum's Outline Series, McGraw-Hill Book Co., Inc., N. Y., 359 p.
- Steel, R. G. D., and J. H. Torre, 1960, *Principles and Procedures of Statistics*, McGraw-Hill Book Co., Inc., N. Y., 481 p.
- Willey, R. L., 1972, Physical and Geological Aspects of Heiligenschien Measurements, in *Apollo 16 Preliminary Science Report*: NASA SP-315, Part Y, p. 29 (113)-29 (115).
- Wu, S. S. C., and H. J. Moore, 1972, Frequency distributions of lunar slopes, in *Apollo 16 Preliminary Science Report*: NASA SP-315, Part C, p. 30(10)-30(15).
- Wu, S. S. C., F. J. Schafer, G. M. Nakata, and R. Jordan, 1973, Repeatability of Elevation Measurements-Apollo Photography, in *Apollo 17 Preliminary Science Report*, Part D, Natl. Aeronautics and Space Admin. Spec. Publ., NASA SP-330, p. 33(35)-33(40).

BOOK REVIEWS

Image Science—principles, analysis and evaluation of photographic-type imaging processes, J. C. Dainty and R. Shaw, Academic Press, NY (1974), 16×23.5 cm, 232 illus. pp xiv & 402. \$26.00 hard.

Military requirements, the great space explorations, and the introduction of commercial television gave enormous impetus to the development of image science from 1940 to 1970. Psychophysics became an established interdisciplinary, information theory developed, and optical scientists learned how to treat problems in that great no-man's-land between coherence and incoherence. Facts and theories were reported in scattered journals, special publications, interim and final reports (some still classified), or not documented at all. Now, Dainty and Shaw have gathered up the pieces, organized them as they have never been organized before, and established a uniform body of image science.

Since their book is the only one of its kind, no direct comparisons can be drawn. There is simply too much subject matter in this field to include it in a general optics book. Their book is a thoroughly competent text, well organized and well written. The level is typical of a junior or senior year physics text. The problems at the end of each chapter are interesting and relevant to practice. The principles they treat are applicable to other imaging processes, such as television, but much of the emphasis is on photographic systems, as the subtitle indicates. Most studies have dealt with photography and it provides a handy embodiment of an image for discussion. This is not a book about how images are formed but about the principles